



Published in final edited form as:

*Nanotechnology*. 2011 November 04; 22(44): 445101. doi:10.1088/0957-4484/22/44/445101.

## Efficient nanoparticle mediated sustained RNA interference in human primary endothelial cells

Anindita Mukerjee, Jwalitha Shankardas, Amalendu P. Ranjan, and Jamboor K. Vishwanatha

Department of Molecular Biology & Immunology and Institute for Cancer Research, Graduate School of Biomedical Sciences, University of North Texas Health Science Center, Fort Worth, Texas, 76107, USA

### Abstract

Endothelium forms an important target for drug and/or gene therapy since endothelial cells play critical roles in angiogenesis and vascular functions and are associated with various pathophysiological conditions. RNA-mediated gene silencing presents a new therapeutic approach to overcome many such diseases. But the major challenge of such an approach is to ensure minimal toxicity and effective transfection efficiency of shRNA to primary endothelial cells. In the present study, we formulated shAnnexin A2 loaded PLGA nanoparticles which produced intracellular siRNA against Annexin A2 and brought about the downregulation of Annexin A2. The percent encapsulation of the plasmid within the nanoparticle was found to be 57.65%. We compared our nanoparticle based transfections with lipofectamine mediated transfection and our studies show that nanoparticle based transfection efficiency is very high (~97%) and is more sustained as compared to conventional lipofectamine mediated transfections in primary retinal microvascular endothelial cells and human cancer cell lines. Our findings also show that the shAnnexin A2 loaded PLGA nanoparticles had minimal toxicity with almost 95% cells being viable 24 hours post transfection while lipofectamine based transfections resulted in only 30% viable cells. Therefore, PLGA nanoparticle based transfection may be used for efficient siRNA transfection to human primary endothelial and cancer cells. This may serve as a potential adjuvant treatment option for diseases such as diabetic retinopathy, retinopathy of prematurity and age related macular degeneration besides various cancers.

### Keywords

Nanoparticle; PLGA; Cancer; Annexin A2; siRNA

### 1. Introduction

Endothelial cells play vital roles in the regulation of vascular permeability and angiogenesis which is a complex, multistage process responsible for the formation of new blood vessels

\* *Corresponding Author*. Dr. Jamboor K. Vishwanatha, Dean and Professor, Department of Molecular Biology & Immunology, Director, Institute for Cancer Research, Graduate School of Biomedical Sciences, University of North Texas Health Science Center, Fort Worth, Texas 76107, USA, Phone: 817-735-0477, Fax: 817-735-0243, Jamboor.vishwanatha@unthsc.edu.

[1]. Angiogenesis plays an important role in wound healing, embryonic development, and in several pathological conditions including diabetic retinopathy and the growth and metastasis of tumor cells [2–4]. The regulation of angiogenesis, both by enhancement or inhibition, has important clinical applications and has therefore been one of the focal targets for gene therapy. Specific post-transcriptional silencing of genes associated to disease using exogenous short interfering RNA (siRNA) [5, 6] has been a promising strategy in gene therapy. siRNA is known to modulate enzymatic-induced cleavage of homologous mRNA and subsequently interrupt gene expression (RNA interference).

Clinical application of siRNA in endothelial cells has two major limitations: first, siRNA treatment gets hampered by its rapid degradation, poor cellular uptake, non-specific distribution and low endosomal escape efficiency [7, 8]. Second, using siRNA with endothelial cells is not amenable to molecular genetic modifications because of the difficulty of effectively transfecting primary cells. Transfection efficiencies in endothelial cells using standard calcium phosphate, DEAE-dextran, or cationic liposome techniques have not exceeded 20–30% [9, 10]. Further, effective and safe gene delivery to primary endothelial cells in the presence of serum proteins is known to be particularly challenging. Efficiencies exceeding 90% have been observed with adenovirus vectors [11, 12], but the utility of viral vectors is limited by small cargo capacity, resistance to repeated infection, safety issues like acute toxicity, cellular immune response, and oncogenicity due to insertional mutagenesis, and quality control. Therefore, the ability to transiently transfect endothelial cells with high efficiencies with siRNA is essential for successful development of siRNA-based therapeutics. To this end, nanoparticle based delivery systems are increasing becoming popular as they protect and transport siRNA to reach its site of action in the cytosol. Such non-viral delivery systems also overcome many of the obstacles inherently associated with the administration of plasmid DNA and RNAi with viral vectors [13–19]. The present investigation was designed to develop a high-efficiency technique for reliable transient transfection of primary endothelial cells for siRNA therapy using PLGA nanoparticles as they provide excellent transfection capabilities in cancer cells [20]. PLGA nanoparticles for delivery of therapeutics are advantageous as they are biocompatible, biodegradable and have the ability to maintain therapeutic drug levels for sustained periods of time. The polymer matrix prevents the degradation of the siRNA and the duration and levels of siRNA released from the nanoparticles can be easily tailored by altering the formulation parameters. These properties of protection and long-term sustained-release are of particular interest for siRNA therapeutics, since the RNA backbone is more susceptible to serum nuclease hydrolysis than DNA, and the silencing effects of siRNA are transient [21].

In this study, Annexin A2 was chosen as the therapeutic target for siRNA therapy as over-expression of annexin A2 is found to play an important regulatory role in neo-angiogenesis [22, 23], cellular proliferation [24], extracellular matrix organization [25], fibrinolysis and migration [26]. Annexin A2 is an important member of a Ca<sup>2+</sup> binding and cellular membrane associated family of proteins abundantly expressed in most cancers [25, 27]. Another area of interest where neovascularization has debilitating consequences is in the diseases of the eye such as diabetic retinopathy, retinopathy of prematurity and age related macular degeneration [28]. Therefore, we formulated shAnnexin A2 loaded PLGA nanoparticles, which upon transfection and cellular uptake produced siRNA against Annexin

A2 and subsequently downregulated Annexin A2 in primary retinal microvascular endothelial cells as well as in human prostate and breast cancer cell lines. To our knowledge, it is for the first time that nanoparticle mediated delivery of shAnnexin A2 to human primary cells has been successfully studied.

## 2. Material and Methods

### 2.1 Materials

Poly(D,L-lactide-co-glycolide) 50:50; i.v. 1.13 dL/g; mw 50,000 was purchased from Absorbable Polymers International (Pelham, AL). Polyvinyl alcohol (mw 30,000–70,000), collagenase, Nile red, trypan blue and Luria broth were purchased from Sigma Aldrich (Sigma, St. Louis, MO). RPMI 1640 media, DMEM media, FBS and trypsin-EDTA was obtained from Gibco, Invitrogen, CA, USA. EGM2-MV media was purchased from Lonza, Allendale, NJ. Qiagen<sup>®</sup> Maxi prep kit was purchased from Qiagen, CA, USA. Lipofectamine<sup>™</sup> 2000 Transfection Reagent, Gold antifade mounting agent with DAPI, magnetic CD31 Dynabeads, DynaMag<sup>™</sup>-15 magnet were purchased from Invitrogen, CA, USA. Fibronectin coated flasks were obtained from Fisher Scientific, Pittsburgh, PA. Annexin A2 antibody and Matrigel basement membrane was purchased from BD Biosciences, San Jose, CA, USA. TNF  $\alpha$  was obtained from R&D Systems, Minneapolis, MN, USA. pGIPZ vector and shAnnexin A2 plasmid was obtained from Open Biosystems and Thermo Scientific, AL, USA. Double distilled deionized water was used for all the experiments.

### 2.2 Amplification and isolation of shAnnexin A2 plasmid from *E. coli*

pGIPZ vector and shAnnexin A2 plasmid were amplified in *E. coli* grown in Luria broth (LB) medium and plasmid DNA was then isolated using Qiagen<sup>®</sup> maxi prep using manufacturer's protocol.

### 2.3 Nanoparticle Formulation

PLGA nanoparticles loaded with shAnnexin A2 were formulated using w/o/w emulsion technique. The formulation was optimized by varying the polymer concentration, volume ratio between the internal aqueous phase and organic phase and plasmid concentration. Briefly, 30mg of the polymer PLGA was dissolved in 1 ml of ethyl acetate. 100 $\mu$ l of the plasmid was added to the PLGA/ethyl acetate solution (kept on ice) and sonicated at 55W for 30 seconds in a Branson Sonifier model W-350 (Branson, Danbury, CN) to produce the water-in-oil emulsion. This emulsion was then added to a solution of 1% PVA (kept on ice) and again sonicated at 55W for 1.5 minutes to form the water-oil-water double emulsion. This emulsion was then centrifuged at 15,000g for 25 minutes to assist the removal of residual solvents. The nanoparticles thus obtained were washed three times with deionized distilled water. They were then freeze dried and lyophilized for 24 hours on an ATR FD 3.0 system (ATR Inc., St. Louis, MO.). The nanoparticles were stored at 4°C until further use.

For preparing fluorescent nanoparticles, a 1mg/ml aqueous stock solution of Nile red was prepared. From the stock solution, 10 $\mu$ l of Nile red was added to a PLGA/chloroform

solution and the formulation was carried out as described earlier. The labeled nanoparticles were stored in the dark at 4°C until used in experimentation.

## 2.4 Nanoparticle Characterization

The nanoparticles formed were characterized for percent entrapment, particle size distribution and surface morphology. The encapsulation efficiency of the nanoparticles was determined by analyzing the supernatant of the final emulsion, once the nanoparticles were removed from it, by centrifugation at 15,000g for 15 minutes. For the estimation of plasmid present in the supernatant, absorbance was measured in a spectrophotometer at 260nm. The amount of the drug encapsulated and the percent encapsulation in the nanoparticles is given by:

$$\text{shRNA(encapsulated)} = \text{shRNA(total)} - \text{shRNA(filtrate)}$$

$$\% \text{ Encapsulation} = \frac{\text{shRNA(encapsulated)}}{\text{shRNA(total)}} \times 100$$

Particle size analysis of the shRNA loaded nanoparticles was carried out using the Nanotracs system (Mircotrac, Inc., Montgomeryville, PA). The lyophilized nanoparticles were dispersed in aqueous buffer using an ultrasonic water bath (Fisher Scientific, USA) for 30 seconds and then measured for particle size. The results were reported as average of five runs with triplicates in each run.

The surface morphology of the nanoparticles was studied using transmission electron microscopy (TEM). A small quantity of aqueous solution of the lyophilized shRNA loaded nanoparticles (1mg/ml) was placed on the grid surface with a filter paper (Whatman No. 1). A drop of 1% uranyl acetate was added to the surface of the carbon coated grid which acts as the negative stain. After 1 minute of incubation, excess fluid was removed and the grid surface was air dried at room temperature. It was then loaded in the transmission electron microscope (LEO EM910, Carl Zeiss SMT Inc, NY, USA) attached to a Gatan SC 1000 CCD camera.

The release of plasmid from shAnnexin A2 loaded PLGA nanoparticles were measured in TE buffer. Briefly, a known amount of lyophilized shAnnexin A2 loaded PLGA nanoparticles (50 mg) were dispersed in 5 ml TE buffer. The solution was divided in RNase-free microcentrifuge tubes (500µl each). The samples were kept in an orbital shaker (Cellstar, USA) maintained at 37°C ± 0.5°C stirring at 50 rpm. At specified time intervals, the tubes were centrifuged (15,000g for 15 min) and the supernatants were collected. Samples were taken and analyzed in triplicates. The concentration of shAnnexin A2 was determined from the corresponding absorbance measured in a spectrophotometer at 260nm.

## 2.5 Isolation and culture of retinal microvascular endothelial cells (RMVEC)

All tissue samples were obtained in compliance with good clinical practice, with informed consent under Institutional Review Board (IRB) regulations, and also in accordance with the tenets of the Declaration of Helsinki.

The endothelial cells were isolated by modification to a previously described protocol [29]. Briefly, a 10mm diameter punch biopsy was removed from the macula of the donor retina. The sample was removed and the retinal pigment epithelium (RPE) removed by gentle brushing with a sterile spatula and washed twice with sterile phosphate buffered saline (PBS). The tissue was then digested using collagenase (2mg/ml) for 1 hour with constant agitation. The RMVECs were separated from the underlying retinal pigment epithelial cells (RPEs) using magnetic CD31 Dynabeads according to manufacturer's instructions. The CD31 positive RMVECs that bound to the Dynabeads were isolated from the cell suspension using a magnet. The cells bound to the Dynabeads were washed and re-suspended in endothelial growth medium (EGM2-MV) and seeded onto fibronectin (FNC) coated 25cm<sup>2</sup> flasks or 6-well plates. Isolated human RMVECs were tested by immunofluorescence analysis for expression of endothelial cell markers and their ability to form capillary tubes by seeding them on matrigel basement membrane. Formation of capillary tube like structures was noticed 12 to 24hrs following cell seeding on matrigel.

Primary RMVEC cells were maintained at 37°C in 5% CO<sub>2</sub>. For progressive passages, cells were trypsinized with 0.05% trypsin-EDTA and cultured in FNC coated 60mm dishes. The isolated RMVECs can be progressively passaged for up to 6–8 passages and they retain their morphological and physiological properties. The experiments performed in this study utilized primary RMVEC cells from 3 different donor tissues (Ages: 79, 76 and 80 years).

## 2.6 Culture of cancer cell lines

Human prostate cancer cell line, DU145, was cultured in RPMI 1640 medium with 10% FBS. Human breast cancer cell line, MDA MB 231 was cultured in DMEM medium containing 10% FBS with 1% antibacterial and antimycotic cocktail. The cells were passaged by trypsinizing with 0.05% trypsin-EDTA and cultured in T-25 flasks (VWR International Irving, TX).

## 2.7 Lipofectamine mediated cell transfection

Cells (DU145, MDA MB 231 and RMVEC) were seeded in a 6-well plate at a density of 50–60%. After 12 hours, they were transfected with control plasmid and shAnnexin A2 using Lipofectamine™ 2000 transfection reagent according to manufacturer's protocol.

## 2.8 Nanoparticle mediated cell transfection

Cells (RMVECs, DU145 and MDA MB 231) were seeded in a 6-well plate at a density of 50–60%. Following cell attachment, they were transfected with PLGA nanoparticles encapsulating control plasmid or PLGA nanoparticles encapsulating shAnnexin A2 at a dose concentration of 4µg of shRNA each.

## 2.9 Cytotoxicity Assay

Cells were plated in a 6-well plate at a known cell density (100,000 to 500,000). Following cell attachment, the floaters (unattached cells) were counted following staining with trypan blue and the medium changed. This facilitates determination of the exact seeding density. The cells were transfected as described earlier using lipofectamine or nanoparticles. Twenty four hours following transfection, the number of dead cells in the medium, stained using trypan blue, were counted and the numbers plotted to determine the cytotoxicity.

## 2.10 Intracellular uptake studies

Cellular uptake of shAnnexin A2-loaded Nile red-labeled nanoparticles was determined using Fluorescence microscope (Olympus-Provis, AX70) attached to an Olympus camera (DP70 Digital). For these experiments, approximately 15,000 cells were plated on glass coverslips (12 cm<sup>2</sup>, Thermofisher, Fisher Scientific, Pittsburgh, PA) and cultured in their respective media. The cells were then exposed to 100µg/ml concentrations of shAnnexin A2 loaded labeled nanoparticles. At time points of 24 hour and 48 hours, the coverslips were rinsed in PBS after which 100µl of 4% paraformaldehyde was added to each well and kept for 30 minutes. The cells were then washed twice with PBS and mounted on slides with Gold antifade mounting agent with 4', 6-diamino-2-phenylindole (DAPI). These cells were viewed under the microscope to determine the extent of intracellular uptake of DNA-lipofectamine complex or nanoparticles.

## 2.11 Downregulation of Annexin A2 by Western blot analysis

Cultured cancer cell lines and primary cells were lysed at different time points following transfection (24, 48, 72 and 96 hours). Both controls and transfected cells were treated with lysis buffer [2.5ml 1M Tris buffer (pH = 7.0), 1g SDS, and 2.5g sucrose in 50ml distilled water] for 5 minutes at room temperature. Genomic DNA was sheared by several passes through a 22-gauge needle, and samples stored at -20°C until needed. BCA protein assays (Pierce, Rockford, IL) of lysates were performed to determine the protein concentration to ensure equal loading of lanes. SDS PAGE was performed at room temperature (RT), loading 20µg protein/lane using 12% Tris-Glycine, at 150V in Tris/glycine as the running buffer. Protein bands were transferred onto nitrocellulose membranes (VWR International Irving, TX) by electro-blotting (iBlot<sup>®</sup> Gel Transfer System, Invitrogen, CA, USA). After brief washing of the membranes in distilled water, they were blocked for 1 hour at room temperature in blocking buffer (5% powdered milk and 1% BSA in PBS). Membranes were incubated with primary annexin A2 antibody at room temperature for 30 minutes followed by overnight incubation at 4°C. After rinsing the membranes in PBS (3 washes for 10 minutes each), the membranes were incubated with secondary anti-mouse antibody (Promega, WI, USA) for 1 hour, rinsed again with PBS (3 washes for 10 minutes each) and finally developed using ECL chemiluminescence agent (Amersham Biosciences, UK). Glyceraldehyde 3-phosphate dehydrogenase (GAPDH) was used as a loading control for all the blots.

## 2.12 In vitro Angiogenesis Assay

RMVECs were tested for their ability to form capillary tubes by seeding them on matrigel basement membrane. Formation of capillary tube like structures was noticed 12 to 24 hours following cell seeding on matrigel. Unpolymerized Matrigel (17 mg/ml) was placed (50  $\mu$ l per well) in a 96 well microtiter plate (0.32 cm<sup>2</sup> per well) and polymerized for 1 hour at 37°C. RMVEC cells ( $2 \times 10^4$  per well) both control (scrambled plasmid) and transfected (shAnnexin A2 plasmid) cells (72 hours post transfection) in 200  $\mu$ L of EBM medium were seeded onto the Matrigel surface. After 12 and 24 hours of incubation in a 5% CO<sub>2</sub> humidified atmosphere at 37°C, cell growth and three-dimensional organization was observed under a microscope. The number of tubes under each experimental condition was counted and compared with controls.

## 2.13 Wound Healing Assay

The effect of shAnnexin-loaded nanoparticle-mediated annexin A2 expression on cellular migration was studied by the scratch/ wound healing assay in DU145 cells. The cells were grown in 6-well plates till they reached sub confluent levels. They were then treated with shAnnexin loaded nanoparticles. Untreated cells served as controls. After 72 hours of treatment, a scratch was made in all the wells. Microscope pictures were taken at 0 and 24 hours after the scratch was made. The distance between the parallel sides of the wound was quantitated by Image-J software and plotted.

## 2.14 Statistical Analysis

Statistical analysis was performed using paired *t*-test and a p-value <0.05 was taken as statistically significant for all the experiments.

# 3 Results and Discussion

## 3.1 Nanoparticle Formulation and Characterization

The main objective in siRNA therapy is to transfer the genetic material to the tissues successfully *in vivo*. RNA interference in cells is mediated through two types of molecules; the double-stranded small interfering RNA (siRNA) which is chemically synthesized or short hairpin RNA (shRNA) which is vector based. shRNAs, as opposed to siRNAs, are synthesized in the nucleus of cells, where they are processed and then transported to the cytoplasm. These are then incorporated into the RNA-interfering silencing complex (RISC) for activity. The primary transcripts (pri-shRNA) follow a route similar to that of primary transcripts of microRNA which are then processed by the Drosha/DGCR8 complex to form pre-shRNAs. Pre-shRNAs are transported to the cytoplasm via exportin 5. In the cytoplasm the pre-shRNA is loaded onto another RNase III complex containing the RNase III enzyme Dicer and TRBP/PACT where the loop of the hairpin is processed off to form a mature double-stranded siRNA. Argonaute protein containing RISC get associated with this mature shRNA in the Dicer/TRBP/PACT complex and provide RNA interference function by mRNA cleavage and degradation or through translational suppression via p-bodies [30]. However, naked therapeutic genes C get rapidly degraded by nucleases especially *in vivo* in presence of serum. Therefore, the development of gene carriers that are safe and are capable

of high efficiency transfection are absolutely crucial for successful gene therapy. Nanoparticles loaded with shAnnexin A2 were successfully formulated with the double emulsion technique. The formulation was optimized by varying the polymer concentration, volume ratio between the internal aqueous phase and organic phase and plasmid concentration. We found that all these parameters influenced the encapsulation efficiency and particle size (data not shown) of the nanoparticles. The optimized batch of nanoparticles formed was characterized for percent entrapment, particle size distribution and surface morphology. The encapsulation efficiency of the nanoparticles was found to be  $57.65 \pm 1.24\%$  and shAnnexin A2 load was found to be  $3.4\mu\text{g}$  plasmid/mg of PLGA nanoparticles. The low encapsulation can be explained due to the partial leaching of the internal aqueous phase to the external aqueous stabilizer phase. Similar encapsulation efficiencies with w/o/w emulsion technique have been earlier reported [31, 32], while other reports show only 21.5% encapsulation efficiency with PLGA nanoparticles encapsulating siRNA [7]. The particle size for the nanoparticles was determined by dynamic light scattering. Figure 1a depicts a narrow size distribution for shAnnexin A2 loaded PLGA nanoparticles with the mean particle size being 165nm. The surface morphology of the nanoparticles encapsulating shAnnexin A2 was determined by TEM. Figure 1B illustrates a TEM scan showing the formation of spherical and smooth nanoparticles. The scan also reveals that the particles have a relatively uniform size distribution and low polydispersity as also represented by a narrow distribution in Figure 1A.

The release kinetics of shAnnexin A2 plasmid from the PLGA nanoparticles was studied for 120 hours. Plasmid release from PLGA nanoparticles occurs in a biphasic manner with an initial burst phase followed by diffusion controlled slower drug release phase. In our studies, an initial burst phase corresponding to about 13–15% was observed within 1 hour due to desorption and release of plasmid from the nanoparticle surface. A sustained release of the plasmid to a total of about 55% was reported from these nanoparticles over the entire period of study, as depicted in the graph shown in Figure 1C. The sustained release characteristic of PLGA nanoparticles may be engineered by varying parameters such as polymer composition, polymer and stabilizer concentration, particle size, drug/plasmid content and various types of surface modifications [33, 34].

## 3.2 Lipofectamine vs Nanoparticle mediated Transfection

**3.2.1 Intracellular uptake and Transfection efficiency**—Intracellular trafficking, gene silencing and subsequent decrease in protein synthesis are critical parameters that are prerequisites while designing efficient siRNA delivery systems. Internalization of shAnnexin A2 loaded PLGA nanoparticles into cells occur by endocytosis. Internalized particles are trafficked to endosomes followed by endosomal release of these particles and/or the plasmid into cytoplasm. Released shAnnexin A2 plasmid then enters the nucleus to be processed to pre-shRNA and gets transported back to the cytoplasm where they associate with RNA-interfering silencing complex and guide the cleavage of complementary target mRNA in the cytoplasm [35]. This present study was intended to evaluate the ability of shAnnexin A2 loaded PLGA nanoparticles to transfer the gene, shAnnexin A2, to primary endothelial and cancer cells.



Cells (RMVEC, DU145 and MDA MB 231) were transfected with scrambled shRNA (control) and shAnnexin A2 using lipofectamine and shAnnexin A2 loaded nanoparticles. Intracellular uptake and subsequent GFP expression of shAnnexin A2 loaded with nanoparticles, almost all cells, whether primary or cancer, show a very robust cellular uptake and efficient transfection. A very high transfection efficiency was observed with nanoparticles loaded with shAnnexin A2 plasmid in both primary endothelial as well as cancer cells (Figure 2).

Intracellular uptake of fluorescent-nile red labeled nanoparticles in cells makes the cells appear red. It is evident from the images that nanoparticle mediated transfection efficiency is substantially higher (~97%) as seen by the number of cells expressing GFP (appearing green) as a result of transcription and translation of shAnnexin A2 plasmid both at 24 and 48 hours as compared to ~60% transfection efficiency obtained with lipofectamine. This result is of particular interest since it is very difficult to successfully transfect primary cells in culture with commercially available transfecting agents like lipofectamine. This finding also confirms the functional integrity of the plasmid during its encapsulation and subsequent release from the nanoparticles. Much research has been carried out to find a procedure to transfect primary cells successfully but none have shown high transfection efficiency. Yu et al studied transfection characteristics of LHLN and CTAB-SLN to transfer reporter gene, EGFP, to A549 lung cancer and HeLa cervical cancer cells [36]. Their results show that naked DNA could barely transfect either A549 cells or HeLa cells, while Lipofectamine–DNA, LHLN-DNA and CTAB-DNA complexes could more or less achieve the intracellular gene transfection. However, the transfection efficiency of LHLN SLN–DNA complexes was lower than that of Lipofectamine–DNA complexes at 24 hours while similar transfection efficiency was obtained at 48 hours. When compared with their CTAB particles, LHLN modified SLN–DNA complexes gained higher transfection efficiency in both A549 and HeLa cells after 48 hours of transfection. When siRNA was transfected to human glioblastoma cells, U87-luc, using dendritic nanocarriers, PG-PEHA or PEI-PAMAM, the authors reported morphological changes like decreased spreading of cells and disruption of actin fiber morphology even after 5 hours of incubation [37]. With our nanoparticles, we observed cellular uptake within 2 hours of incubation and there were no morphological changes observed in any cell type.

Nanoparticle size also plays a role in cellular uptake and in most cell lines, it has been found to be optimal at around 200nm size [38–40]. We have previously prepared nanoparticles from 50nm to 300nm for other studies [20, 41] and have always seen robust intracellular uptake in this particle size range.

**3.2.2 Cytotoxicity Studies**—A major limitation of using transfection agents like lipofectamine is the high toxicity. Having shown that our shAnnexin A2 loaded nanoparticles efficiently deliver shAnnexin A2 into the cells, we next evaluated its toxicity. Our results showed that cells transfected with lipofectamine showed higher cytotoxicity in a 24 hour time period while nanoparticle mediated transfection showed almost no cytotoxicity. Control cells (transfected with scrambled plasmid) in all cell types showed no cytotoxicity with nanoparticle mediated transfection. In both primary RMVEC cells and cancer cells transfected, the number of viable cells was  $94 \pm 3.2\%$  with shAnnexin A2 loaded nanoparticle

transfection as compared to only  $30 \pm 1.8\%$  viable cells with lipofectamine (Figure 3). There was a slight difference ( $\sim 2\%$ ) observed in viability of cells transfected with shAnnexin A2 loaded nanoparticles between cancer and primary cells. This may be attributed to the fact that primary cells are more sensitive to changes in environment than cancer cells. Similar results were reported by Yu et al stating that LHLN-SLN particles were less cytotoxic than Lipofectamine 2000 in lung and cervical cancer cells [36]. However, these particles did have some cytotoxicity since cationic nanoparticle formulations could lead to considerable toxicity as it may affect cell proliferation, differentiation and may induce necrosis and apoptosis. Other researchers using non-viral transfection procedures have reported cytotoxicity. Ofek et al have reported high toxicity with their dendritic nanocarriers with IC50 for PEI-PAMAM to be as low as  $12 \mu\text{g/ml}$  for human glioblastoma cells [37].

### 3.3 Downregulation of Annexin A2 using lipofectamine and nanoparticle mediated transfection

When primary endothelial RMVEC and DU145 cancer cells were treated with shAnnexin A2 loaded nanoparticles, we see efficient downregulation of Annexin A2 from 48–96 hours in DU145 cells implying significant and sustained downregulation (decrease) in Annexin A2 expression as compared to lipofectamine treatments at these time points. This sustained downregulation is attributed to diffusion dependent slower and sustained release of shAnnexin A2 from the nanoparticles which is reflected by sustained downregulation of Annexin A2 till 96 hours. In primary RMVEC cells, there is a significant decrease in Annexin A2 expression at 72 hours following nanoparticle mediated transfection as seen in Figure 4. No change is observed in the expression levels of Annexin A2 when transfected with scrambled shRNA plasmid (control) with either nanoparticle or lipofectamine mediated transfection. These results emphasize that shAnnexin A2 released from the nanoparticles is able to bring about efficient gene knock down even in primary endothelial cells over a period of time. Yu et al have showed similar sustained release of DNA from their LHLN and CTAB-SLN particles for 3 days in cancer cells [36].

### 3.4 Effect of nanoparticle mediated Annexin A2 downregulation on invasion characteristics of DU145 cells

Formation of new blood vessels and metastasis are two processes that are central to the progression of cancer [42]. Annexin A2 is reported to be an endothelial cell reporter which provides binding sites for plasminogen and tPA for efficient plasmin generation [43, 44]. Many reports have shown that cell surface annexin A2 regulates plasmin generation which in turn facilitates extracellular matrix degeneration, cell invasion [45] and migration [46] and thus plays an important role in neoangiogenesis [22]. The *in vitro* scratch assay is a direct method to study cell migration/invasion *in vitro* since when a new wound is made on a confluent cell monolayer, the cells on the edge of the newly created wound move towards the opening to close the wound until new cell–cell contacts are established again [47]. In our study, the wound healing assay results clearly indicate that there was a decrease in wound closure when DU145 cells were treated with shAnnexin A2 loaded nanoparticles as compared to the untreated cells. In the control untreated cells, the percent wound closure was about 60% while the cells treated with shAnnexin A2 loaded nanoparticles showed about 40% wound closure (Figure 5a). This result emphasizes that shAnnexin A2 released

from the nanoparticles are functionally active to bring about decrease in annexin A2 expression and subsequently decrease in invasion capability of the cancer cells.

### 3.5 Effect of nanoparticle mediated Annexin A2 downregulation on *in vitro* angiogenesis

Endothelial cells are a key player in angiogenesis and are capable of forming capillary tube like structures *in vitro* when in a 3-dimensional environment. Annexin A2 has been shown to play an important role in regulation of homeostasis and neovascularization *in vivo* [22, 43]. Annexin A2 knock down has been shown to decrease neovascularization *in vivo* [22, 48]. *In vitro* angiogenesis assay on matrigel is a commonly used tool to study factors playing a role in angiogenesis and neovascularization. In our study, we have utilized this assay to study the functional effect of the down-regulation of Annexin A2 on tube formation by RMVEC cells. RMVEC cells when seeded on matrigel form capillary tube like structures as shown in Figure 5b. The phase contrast images show the presence of these structures 12–24 hours following cell seeding. The control RMVEC were seeded on matrigel and subject to different experimental conditions- (EBM - complete endothelial culture medium), TNF $\alpha$  (EBM containing 10ng/ml TNF $\alpha$ ), DMEM containing 10% fetal bovine serum (served as the negative control). The RMVEC cells transfected with shAnnexin A2 loaded PLGA nanoparticles were plated on matrigel 72 hours following transfection. The 72hr time point was chosen for this assay because maximum down-regulation of the annexin A2 protein was observed at this time point (as shown in Figure 4). These cells were treated with EBM (complete endothelial culture medium) following attachment to the matrigel. The percentage tube formation was calculated based on the number of cells seeded. Under normal culture conditions, 60% of the seeded RMVEC cells form capillary tube like structures (Figure 5b). In the presence of 10ng/ml TNF $\alpha$ , 95% tube formation is observed as seen in Figure 5b. TNF $\alpha$  is a proangiogenic factor which was used as a positive control for *in vitro* tube formation by RMVEC cells [49]. In the negative control, the RMVEC cells did not form capillary tube like structures on matrigel. RMVEC cells with transfected with shAnnexin A2 plasmid showed significant decrease in tube formation as compared to control cells (EBM complete and TNF $\alpha$  treated). Only 18% of the cells form capillary tube like structures while 60% of the control cells form capillary structures under the same conditions. These results therefore show that effective down-regulation of annexin A2 using PLGA nanoparticles decreases the ability of RMVEC cells to form capillary tube like structures.

## 4 Conclusion

Primary endothelial cells are particularly very difficult to transfect and therefore, an electroporator or a nucleofector is used [37]. In this study, we demonstrate that by using our PLGA nanoparticles loaded with shAnnexin A2, we achieved robust cellular uptake and high transfection efficiency in human primary endothelial as well as cancer cells even with a plasmid size as big as 11.7kb. The encapsulation efficiency of shAnnexin A2 plasmid in the nanoparticles was  $57.65 \pm 1.24\%$  and a mean particle size of 165 nm. Western blot analysis results revealed that nanoparticle based siRNA transfection is more efficient and sustained than the conventional lipofectamine mediated transfection in both primary and cancer cells. Functional assays (wound healing and tube formation assays) confirmed that shAnnexin A2 released from the nanoparticles maintained its functional integrity. These nanoparticles

showed almost no cytotoxicity. Our findings suggest that the use of these sustained-release polymeric nanoparticles for down-regulation of annexin A2 expression may serve as an effective adjuvant treatment option various cancers and in diabetic retinopathy, retinopathy of prematurity and age related macular degeneration. Our future studies will focus on surface modification of our nanoparticles with various ligands to achieve active targeting to specific tissues and cells.

## Acknowledgments

This research was supported in parts by grants from the Department of Defense Breast Cancer Research Program (BC075097), National Institutes of Health (R21CA109593) to Dr. Jamboor K. Vishwanatha and Susan G. Komen Post Doctoral Fellowship (KG101213) to Anindita Mukerjee.

## References

1. Kovala AT, Harvey KA, McGlynn P, Boguslawski G, Garcia JG, English D. High-efficiency transient transfection of endothelial cells for functional analysis. *FASEB J*. 2000 Dec; 14(15):2486–2494. [PubMed: 11099466]
2. Folkman J. Angiogenesis in cancer, vascular, rheumatoid and other disease. *Nat Med*. 1995 Jan; 1(1):27–31. [PubMed: 7584949]
3. Risau W. Mechanisms of angiogenesis. *Nature*. 1997 Apr 17; 386(6626):671–674. [PubMed: 9109485]
4. Zetter BR. Angiogenesis and tumor metastasis. *Annu Rev Med*. 1998; 49:407–424. [PubMed: 9509272]
5. Huang C, Li M, Chen C, Yao Q. Small interfering RNA therapy in cancer: mechanism, potential targets, and clinical applications. *Expert Opin Ther Targets*. 2008 May; 12(5):637–645. [PubMed: 18410245]
6. Singh SK. RNA interference and its therapeutic potential against HIV infection. *Expert Opin Biol Ther*. 2008 Apr; 8(4):449–461. [PubMed: 18352849]
7. Cun D, Foged C, Yang M, Frokjaer S, Nielsen HM. Preparation and characterization of poly(DL-lactide-co-glycolide) nanoparticles for siRNA delivery. *Int J Pharm*. 2010 May 5; 390(1):70–75. [PubMed: 19836438]
8. Xie FY, Woodle MC, Lu PY. Harnessing in vivo siRNA delivery for drug discovery and therapeutic development. *Drug Discov Today*. 2006 Jan; 11(1–2):67–73. [PubMed: 16478693]
9. Tanner FC, Carr DP, Nabel GJ, Nabel EG. Transfection of human endothelial cells. *Cardiovasc Res*. 1997 Sep; 35(3):522–528. [PubMed: 9415297]
10. Niebauer J, Dulak J, Chan JR, Tsao PS, Cooke JP. Gene transfer of nitric oxide synthase: effects on endothelial biology. *J Am Coll Cardiol*. 1999 Oct; 34(4):1201–1207. [PubMed: 10520813]
11. Merrick AF, Shewring LD, Sawyer GJ, Gustafsson KT, Fabre JW. Comparison of adenovirus gene transfer to vascular endothelial cells in cell culture, organ culture, and in vivo. *Transplantation*. 1996 Oct 27; 62(8):1085–1089. [PubMed: 8900307]
12. Wrighton CJ, Hofer-Warbinek R, Moll T, Eytner R, Bach FH, de Martin R. Inhibition of endothelial cell activation by adenovirus-mediated expression of I kappa B alpha, an inhibitor of the transcription factor NF-kappa B. *J Exp Med*. 1996 Mar 1; 183(3):1013–1022. [PubMed: 8642242]
13. Cartiera MS, Johnson KM, Rajendran V, Caplan MJ, Saltzman WM. The uptake and intracellular fate of PLGA nanoparticles in epithelial cells. *Biomaterials*. 2009 May; 30(14):2790–2798. [PubMed: 19232712]
14. des Rieux A, Fievez V, Garinot M, Schneider YJ, Preat V. Nanoparticles as potential oral delivery systems of proteins and vaccines: a mechanistic approach. *J Control Release*. 2006 Nov; 116(1):1–27. [PubMed: 17050027]
15. Prego C, Garcia M, Torres D, Alonso MJ. Transmucosal macromolecular drug delivery. *J Control Release*. 2005 Jan 3; 101(1–3):151–162. [PubMed: 15588901]

16. Hans ML, Lowman AM. Biodegradable nanoparticles for drug delivery and targeting. *Current Opinion in Solid State and Materials Science*. 2002; 6(4):319–327.
17. Soppimath KS, Aminabhavi TM, Kulkarni AR, Rudzinski WE. Biodegradable polymeric nanoparticles as drug delivery devices. *J Controlled Release*. 2001 Jan 29; 70(1–2):1–20.
18. Luo D, Saltzman WM. Synthetic DNA delivery systems. *Nat Biotechnol*. 2000 Jan; 18(1):33–37. [PubMed: 10625387]
19. Panyam J, Labhasetwar V. Biodegradable nanoparticles for drug and gene delivery to cells and tissue. *Adv Drug Deliv Rev*. 2003 Feb 24; 55(3):329–347. [PubMed: 12628320]
20. Mukerjee A, Vishwanatha JK. Formulation, characterization and evaluation of curcumin-loaded PLGA nanospheres for cancer therapy. *Anticancer Res*. 2009 Oct; 29(10):3867–3875. [PubMed: 19846921]
21. Gary DJ, Puri N, Won YY. Polymer-based siRNA delivery: perspectives on the fundamental and phenomenological distinctions from polymer-based DNA delivery. *J Control Release*. 2007 Aug 16; 121(1–2):64–73. [PubMed: 17588702]
22. Ling Q, Jacovina AT, Deora A, Febbraio M, Simantov R, Silverstein RL, et al. Annexin II regulates fibrin homeostasis and neoangiogenesis in vivo. *J Clin Invest*. 2004 Jan; 113(1):38–48. [PubMed: 14702107]
23. Valapala M, Thamake SI, Vishwanatha JK. A competitive hexapeptide inhibitor of annexin A2 prevents hypoxia-induced angiogenic events. *J Cell Sci*. 2011 May 1; 124(Pt 9):1453–1464. [PubMed: 21486955]
24. Balch C, Dedman JR. Annexins II and V inhibit cell migration. *Exp Cell Res*. 1997 Dec 15; 237(2):259–263. [PubMed: 9434621]
25. Chiang Y, Rizzino A, Sibenaller ZA, Wold MS, Vishwanatha JK. Specific down-regulation of annexin II expression in human cells interferes with cell proliferation. *Mol Cell Biochem*. 1999 Sep; 199(1–2):139–147. [PubMed: 10544962]
26. Liu J, Rothermund CA, Ayala-Sanmartin J, Vishwanatha JK. Nuclear annexin II negatively regulates growth of LNCaP cells and substitution of ser 11 and 25 to glu prevents nucleocytoplasmic shuttling of annexin II. *BMC Biochem*. 2003 Sep 9; 4:10. [PubMed: 12962548]
27. Vishwanatha JK, Chiang Y, Kumble KD, Hollingsworth MA, Pour PM. Enhanced expression of annexin II in human pancreatic carcinoma cells and primary pancreatic cancers. *Carcinogenesis*. 1993 Dec; 14(12):2575–2579. [PubMed: 8269629]
28. Sharma MC, Sharma M. The role of annexin II in angiogenesis and tumor progression: a potential therapeutic target. *Curr Pharm Des*. 2007; 13(35):3568–3575. [PubMed: 18220793]
29. Browning AC, Gray T, Amoaku WM. Isolation, culture, and characterisation of human macular inner choroidal microvascular endothelial cells. *Br J Ophthalmol*. 2005 Oct; 89(10):1343–1347. [PubMed: 16170129]
30. Rao DD, Vorhies JS, Senzer N, Nemunaitis J. siRNA vs. shRNA: similarities and differences. *Adv Drug Deliv Rev*. 2009 Jul 25; 61(9):746–759. [PubMed: 19389436]
31. Hombreiro Perez M, Zinutti C, Lamprecht A, Ubrich N, Astier A, Hoffman M, et al. The preparation and evaluation of poly(epsilon-caprolactone) microparticles containing both a lipophilic and a hydrophilic drug. *J Control Release*. 2000 Apr 3; 65(3):429–438. [PubMed: 10699300]
32. Hoffart V, Lamprecht A, Maincent P, Lecompte T, Vigneron C, Ubrich N. Oral bioavailability of a low molecular weight heparin using a polymeric delivery system. *J Control Release*. 2006 Jun 12; 113(1):38–42. [PubMed: 16697485]
33. Budhian A, Siegel SJ, Winey KI. Controlling the in vitro release profiles for a system of haloperidol-loaded PLGA nanoparticles. *Int J Pharm*. 2008 Jan 4; 346(1–2):151–159. [PubMed: 17681683]
34. Sahoo SK, Panyam J, Prabha S, Labhasetwar V. Residual polyvinyl alcohol associated with poly(D,L-lactide-co-glycolide) nanoparticles affects their physical properties and cellular uptake. *J Control Release*. 2002 Jul 18; 82(1):105–114. [PubMed: 12106981]
35. Misra S, Hascall VC, De Giovanni C, Markwald RR, Ghatak S. Delivery of CD44 shRNA/ nanoparticles within cancer cells: perturbation of hyaluronan/CD44v6 interactions and reduction in

- adenoma growth in Apc Min/+ MICE. *J Biol Chem*. 2009 May 1; 284(18):12432–12446. [PubMed: 19246453]
36. Yu W, Liu C, Ye J, Zou W, Zhang N, Xu W. Novel cationic SLN containing a synthesized single-tailed lipid as a modifier for gene delivery. *Nanotechnology*. 2009 May 27.20(21):215102. [PubMed: 19423923]
37. Ofek P, Fischer W, Calderon M, Haag R, Satchi-Fainaro R. In vivo delivery of small interfering RNA to tumors and their vasculature by novel dendritic nanocarriers. *FASEB J*. 2010 Sep; 24(9):3122–3134. [PubMed: 20385622]
38. Rejman J, Oberle V, Zuhorn IS, Hoekstra D. Size-dependent internalization of particles via the pathways of clathrin- and caveolae-mediated endocytosis. *Biochem J*. 2004 Jan 1; 377(Pt 1):159–169. [PubMed: 14505488]
39. Win KY, Feng SS. Effects of particle size and surface coating on cellular uptake of polymeric nanoparticles for oral delivery of anticancer drugs. *Biomaterials*. 2005 May; 26(15):2713–2722. [PubMed: 15585275]
40. He C, Hu Y, Yin L, Tang C, Yin C. Effects of particle size and surface charge on cellular uptake and biodistribution of polymeric nanoparticles. *Biomaterials*. 2010 May; 31(13):3657–3666. [PubMed: 20138662]
41. Ranjan AP, Zeglam K, Mukerjee A, Thamake S, Vishwanatha JK. A sustained release formulation of chitosan modified PLCL:poloxamer blend nanoparticles loaded with optical agent for animal imaging. *Nanotechnology*. 2011 Jul 22.22(29):295104. [PubMed: 21693801]
42. Sharma M, Ownbey RT, Sharma MC. Breast cancer cell surface annexin II induces cell migration and neoangiogenesis via tPA dependent plasmin generation. *Exp Mol Pathol*. 2010 Apr; 88(2):278–286. [PubMed: 20079732]
43. Cesarman GM, Guevara CA, Hajjar KA. An endothelial cell receptor for plasminogen/tissue plasminogen activator (t-PA). II. Annexin II-mediated enhancement of t-PA-dependent plasminogen activation. *J Biol Chem*. 1994 Aug 19; 269(33):21198–21203. [PubMed: 8063741]
44. Hajjar KA, Jacovina AT, Chacko J. An endothelial cell receptor for plasminogen/tissue plasminogen activator. I. Identity with annexin II. *J Biol Chem*. 1994 Aug 19; 269(33):21191–21197. [PubMed: 8063740]
45. Brownstein C, Deora AB, Jacovina AT, Weintraub R, Gertler M, Khan KM, et al. Annexin II mediates plasminogen-dependent matrix invasion by human monocytes: enhanced expression by macrophages. *Blood*. 2004 Jan 1; 103(1):317–324. [PubMed: 14504107]
46. Tarui T, Majumdar M, Miles LA, Ruf W, Takada Y. Plasmin-induced migration of endothelial cells. A potential target for the anti-angiogenic action of angiostatin. *J Biol Chem*. 2002 Sep 13; 277(37):33564–33570. [PubMed: 12087108]
47. Liang CC, Park AY, Guan JL. In vitro scratch assay: a convenient and inexpensive method for analysis of cell migration in vitro. *Nat Protoc*. 2007; 2(2):329–333. [PubMed: 17406593]
48. Zhao S, Huang L, Wu J, Zhang Y, Pan D, Liu X. Vascular endothelial growth factor upregulates expression of annexin A2 in vitro and in a mouse model of ischemic retinopathy. *Mol Vis*. 2009 Jun 17.15:1231–1242. [PubMed: 19536308]
49. Kim NH, Jung HJ, Shibasaki F, Kwon HJ. NBBA, a synthetic small molecule, inhibits TNF-alpha-induced angiogenesis by suppressing the NF-kappaB signaling pathway. *Biochem Biophys Res Commun*. 2010 Jan 15; 391(3):1500–1505. [PubMed: 20035721]

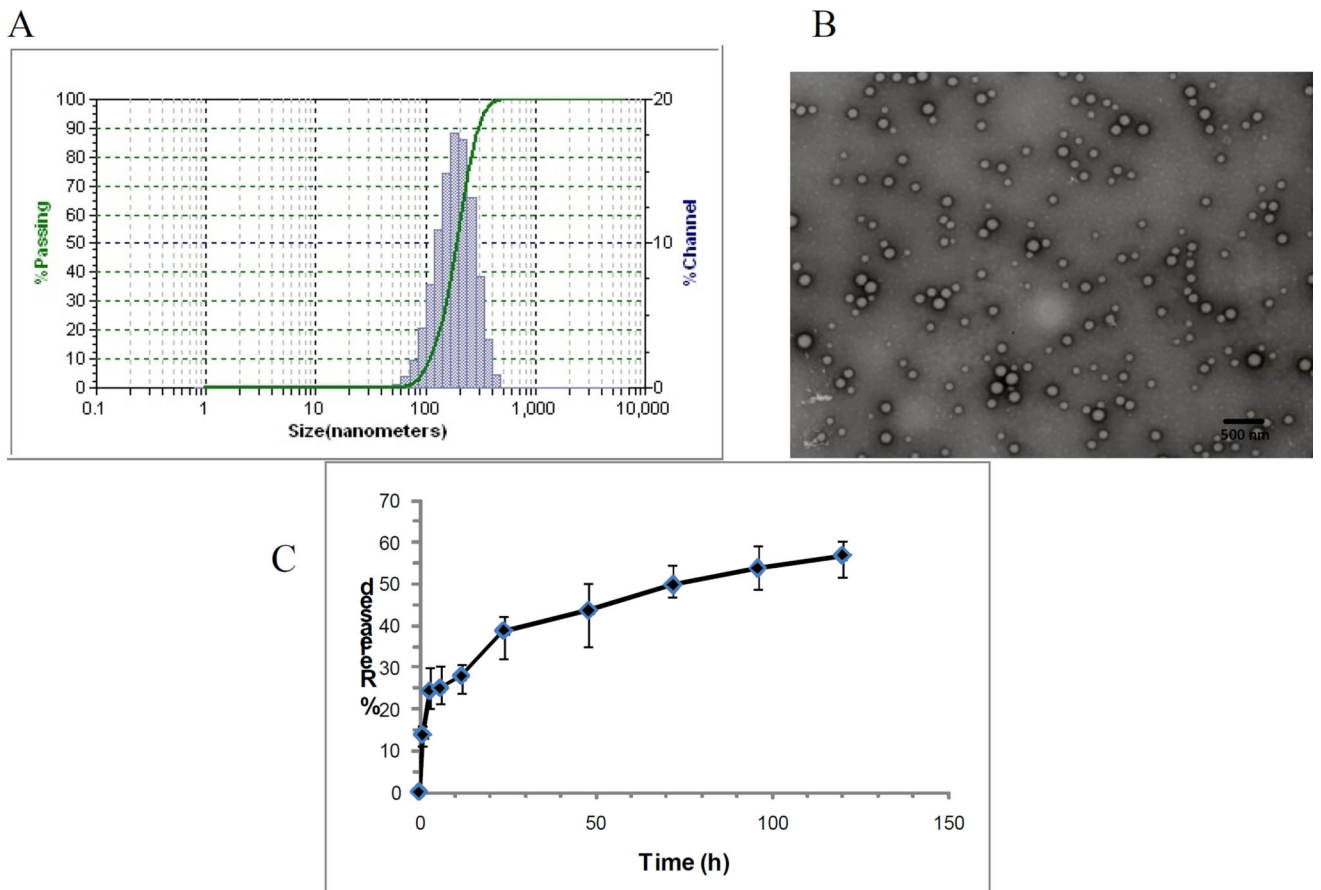
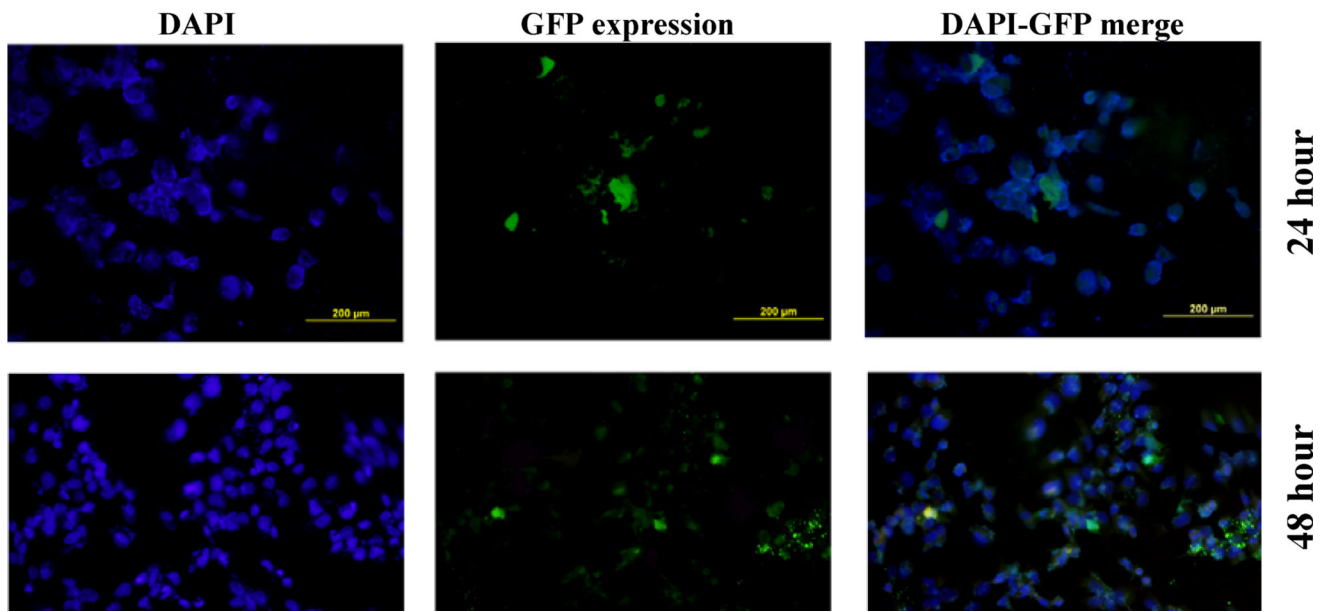


**Figure 1.** A) Particle size analysis; B) Transmission electron microscopy of shAnnexin A2 loaded PLGA nanoparticles; C) Release kinetics of shAnnexin A2 from PLGA nanoparticles

### A) DU145 Cells

#### LIPOFECTAMINE MEDIATED



Author Manuscript

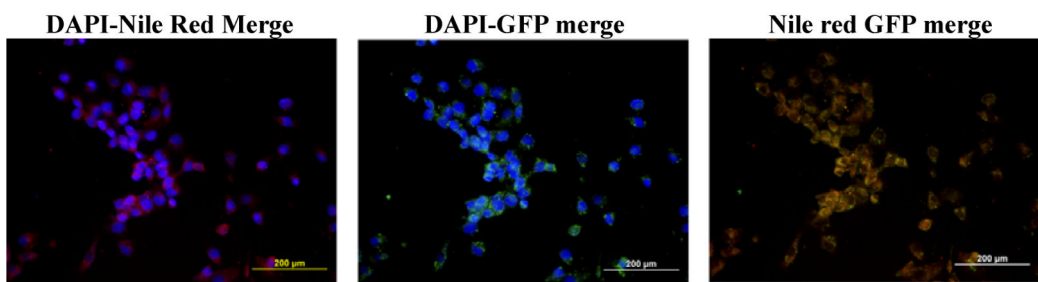
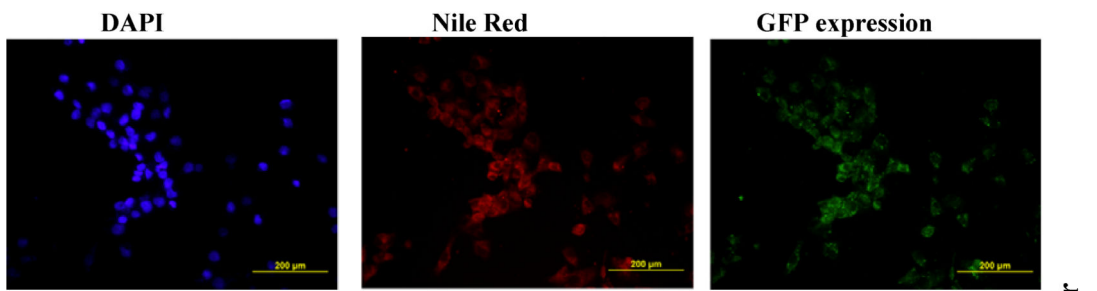
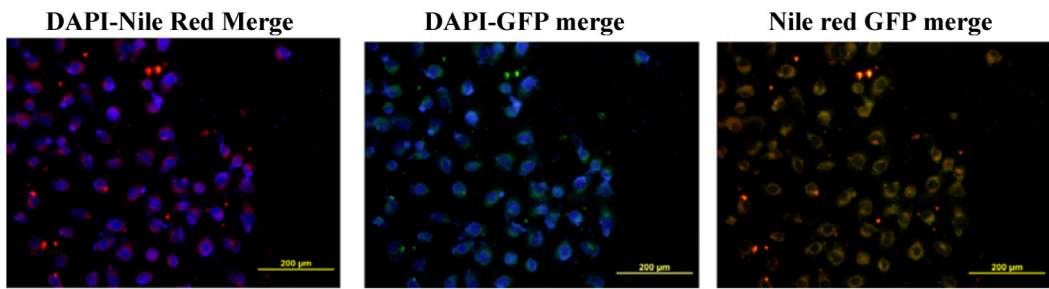
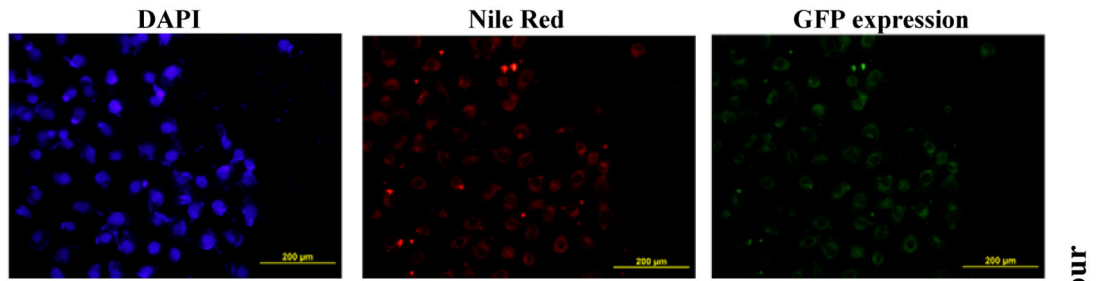
Author Manuscript

Author Manuscript

Author Manuscript

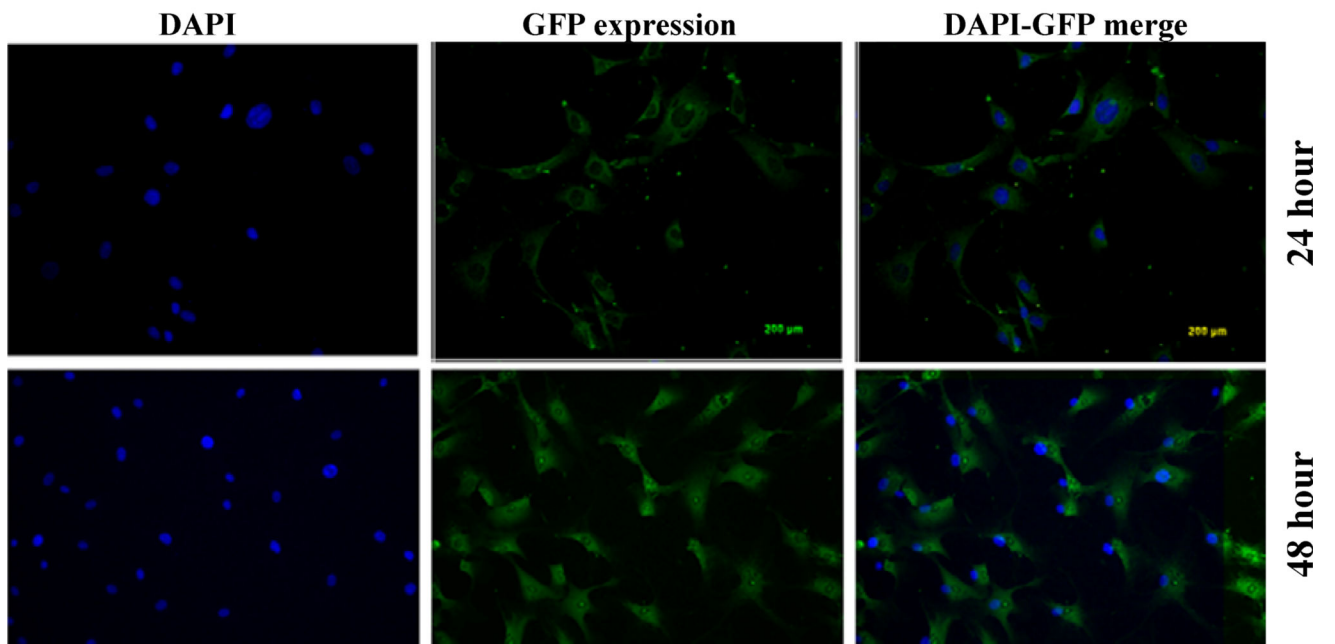


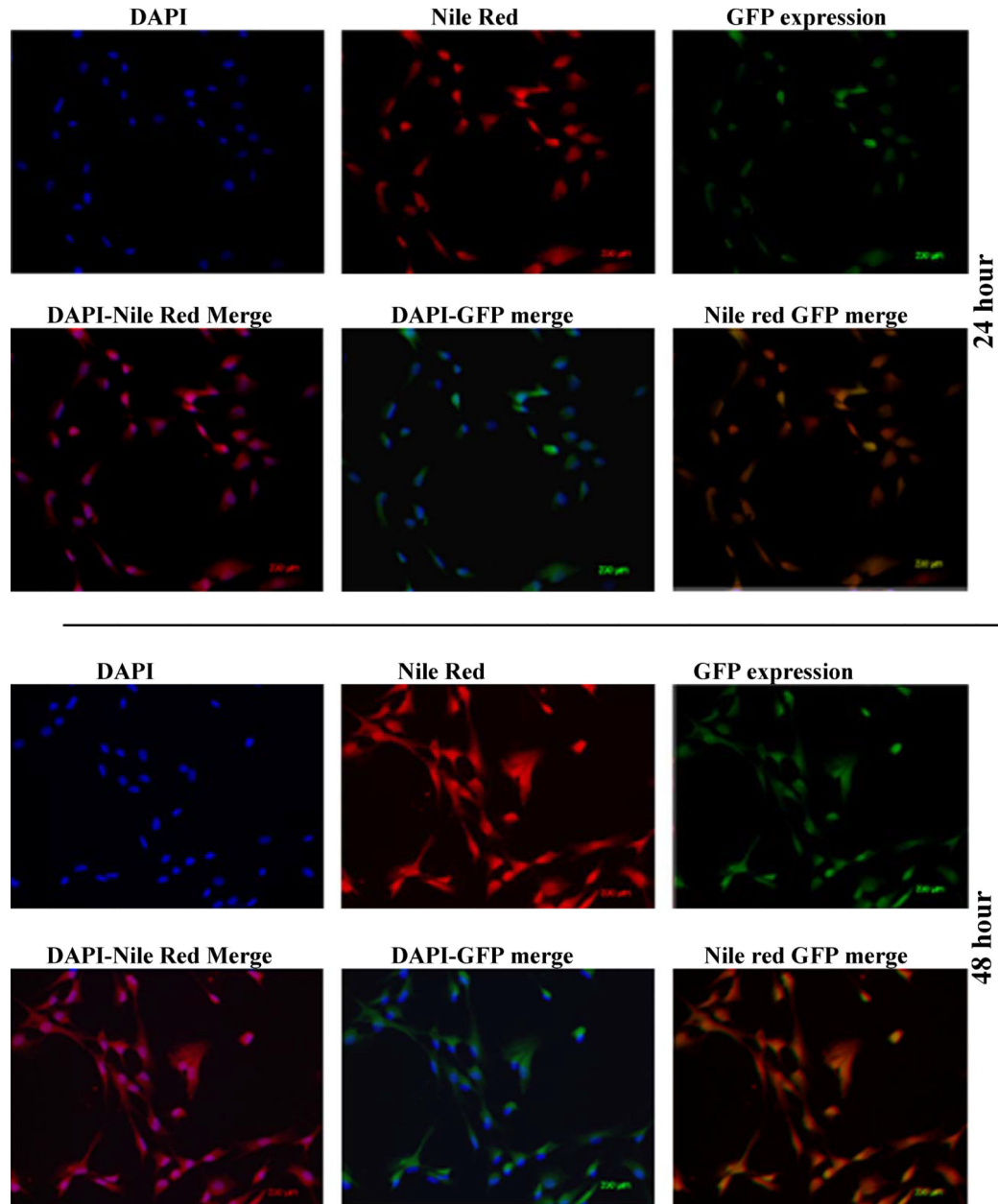
**NANOPARTICLE MEDIATED**



## B) REVEC Cells

### LIPOFECTAMINE MEDIATED



**NANOPARTICLE MEDIATED**

**Figure 2.** Cellular uptake and gene expression A) DU145 cancer cells and B) primary RMVEC cells transfected with Lipofectamine 24 hours following transfection and cells transfected with PLGA nanoparticles 24 hours and 48 hours following transfection.

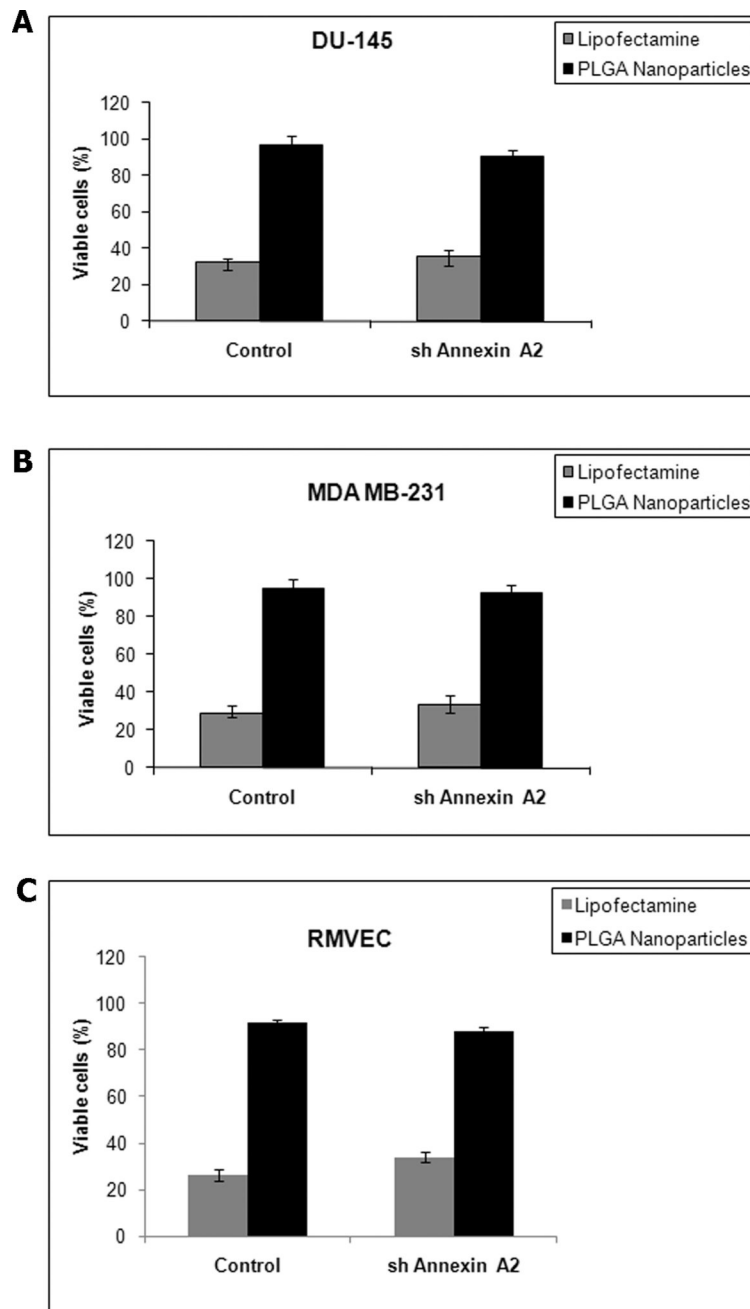


**Figure 3.** Cytotoxicity assay: A) DU145 prostate cancer cells B) MDA MB231 breast cancer cells C) RMVEC primary cells

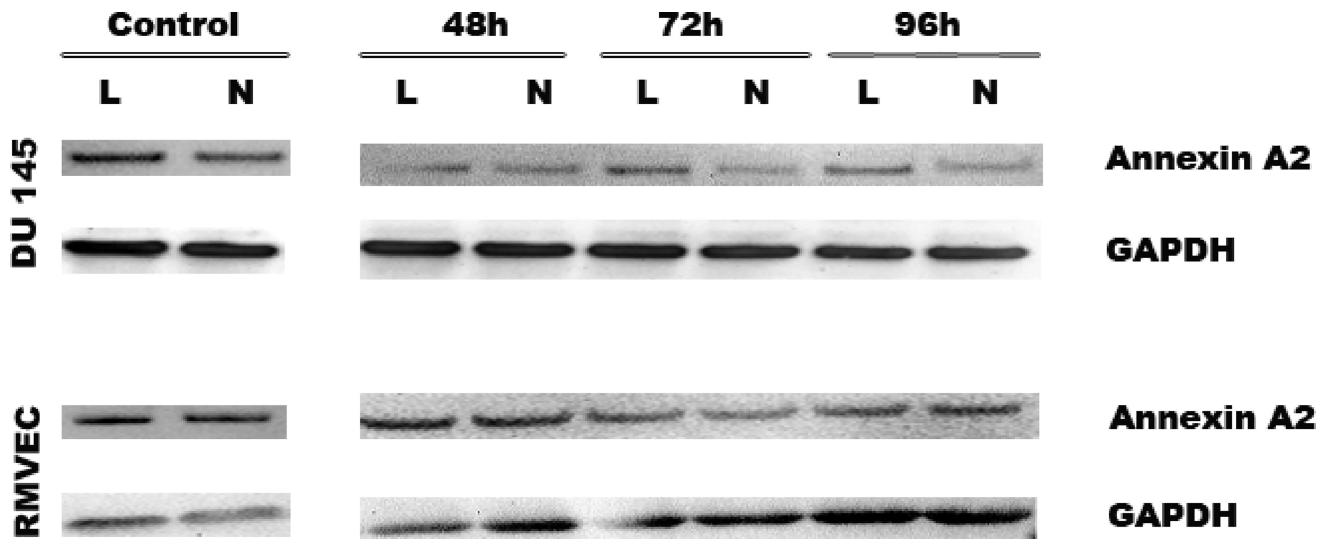


**Figure 4.** Western Blot analysis to determine expression levels of Annexin A2 following lipofectamine and nanoparticle mediated transfection. GAPDH was used as a loading control

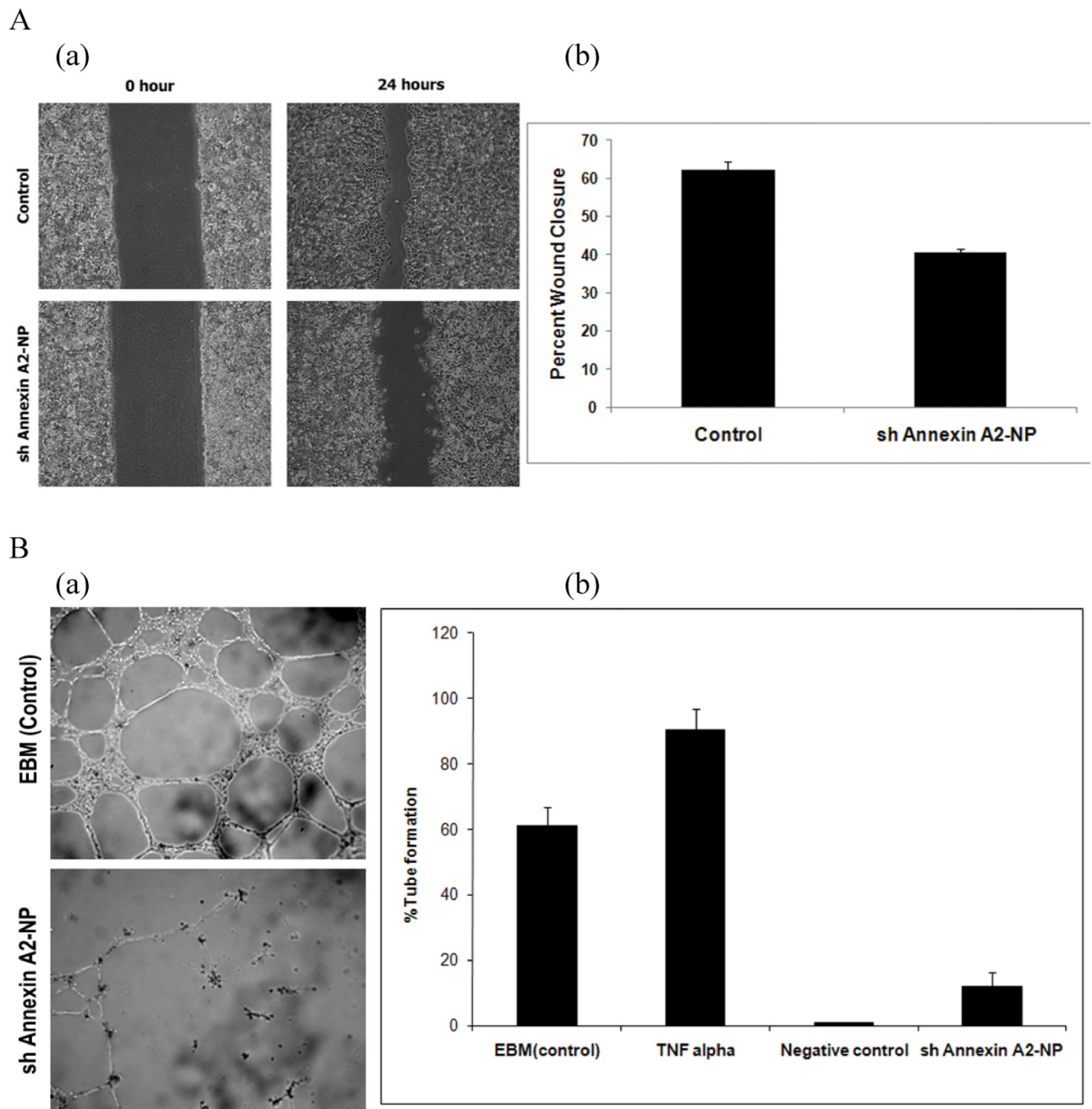


**Figure 5.**

A) Wound healing Assay. (a) Microscopic images of would healing in control (untreated) and shAnnexin-NP treated DU145 cells. (b) Graph representing percent wound closure. B) *In vitro* angiogenesis assay. (a) Phase contrast microscopic image analysis of tube formation of RMVEC (at P2) on matrigel 12 hours after cell seeding (4× magnification). (b) Graphical Representation of angiogenesis assay under normal culture conditions (EBM), 10ng/ml TNF  $\alpha$ , absence of VEGF and DMEM (medium) was used as a negative control.